C-BAND CROSS-POLARIZATION AIRBORNE OCEAN SURFACE NRCS OBSERVATIONS IN HURRICANES: 2015–2019

Joseph Sapp[*]*, Zorana Jelenak*[†]*, Paul Chang*

NOAA/NESDIS/STAR
College Park, MD, USA 20740

Stephen Frasier

University of Massachusetts Amherst
Microwave Remote Sensing Laboratory
Amherst, MA, USA 01003

ABSTRACT

Beginning in 2015, scientists at the National Oceanic and Atmospheric Administration (NOAA)/NESDIS/STAR and UMass Amherst collaborated with the European Space Agency (ESA) to collect ocean surface normalized radar cross-section (NRCS) measurements at co- and cross-polarizations in extreme wind conditions from the NOAA Hurricane Hunter aircraft using a prototype antenna for the next-generation European spaceborne scatterometer. Since then, more research has been done to understand the effects of ocean-surface wind vectors on NRCS from both satellite and aircraft. Here we show the data from several seasons of flight experiments to understand the airborne measurements of NRCS in context.

Index Terms— Sea measurements, C-band, scatterometry, remote sensing, cyclones

1. INTRODUCTION

Since winter 2015, many research flights have been performed on the National Oceanic and Atmospheric Administration (NOAA) WP-3D Hurricane Hunter aircraft in extreme conditions under the direction of scientists at the NOAA/National Environmental Satellite, Data, and Information Service (NESDIS)/Center for Satellite Applications and Research (STAR) Ocean Surface Winds Team (OSWT). The primary instruments in use have been the Imaging Wind and Rain Airborne Profiler (IWRAP) C-band scatterometer [1] and the Stepped Frequency Microwave Radiometer (SFMR)—a C-band radiometer [2] that retrieves ocean-surface wind speed and column-averaged rain rate.

Some of the results of these flight experiments have been presented separately [3]–[5]. IWRAP co- and cross-polarized normalized radar cross-section (NRCS) measurements were investigated, while SFMR retrievals served as ground truth for ocean-surface wind speed and a means of eliminating potentially-rain-contaminated measurements.

[*]Global Science & Technology, Inc.
[†]UCAR

Table 1: Selected Storms Sampled by IWRAP 2015–2019

Season	Experiment	Flights	Saffir-Simpson Category
2015	Patricia (EPAC)	3	TS, 4, 5
2016	Matthew	6	1, 2, 3, 4
2018	Florence	1	4
	Michael	2	1, 3
2019	Dorian	14	TS, 1, 2, 3, 4, 5
	Humberto	1	1
	Lorenzo	1	1

The IWRAP systems were configured the same way as in [4]: a conically-scanning Ku-band antenna and a fixed side-looking C-band fanbeam antenna [6] mounted at 25° off nadir. The antenna used on IWRAP since 2015 is a breadboard prototype for the next-generation MetOp-SG the European Space Agency (ESA) scatterometer. Its benefit over the spinning IWRAP antenna is a cross-polarization isolation sufficiently high to make cross-polarized NRCS measurements of the sea surface possible at wind speeds below $30\,\mathrm{m\,s^{-1}}$ to $40\,\mathrm{m\,s^{-1}}$. In this paper we again focus on the C-band VV and VH measurements, primarily since the MetOp-SG scatterometer will be a C-band instrument with one cross-polarized channel and two co-polarized (VV) channels per swath.

Since the ESA antenna was first put on the NOAA P-3s, more research has been done comparing cross-polarized geophysical model functions (GMFs) and understanding the high-wind cross-polarized NRCS response [7], [8]. The IWRAP measurements augment GMFs derived from satellite analysis with a close time and space collocation inherent to the collocated instruments.

2. METHODOLOGY

Ground calibration of the IWRAP systems were performed before and after the flight experiment season, but an in-flight

calibration still needs to be performed for each set of flights. These calibration values will change from one season to the next due to instrument modifications (e.g., cable and component replacement) despite best efforts to measure the differences. The important factor is that for all of these seasons the ground calibration measurements were the same before and after the season, when accounting for external calibration instrument tolerances.

Table 1 shows information about the conditions in which data presented in this paper was collected. For each season, or row of Table 1, the mean NRCS difference between the CMOD5.h GMF [9] and selected rain-free VV-polarized NRCS between 25 m s^{-1} to 35 m s^{-1} and 30° to 40° was calculated. This value is added to the IWRAP VV NRCS. A similar procedure is done for HH polarization, but using the wind-speed- and incidence-angle-dependent polarization ratio from [10] in addition to CMOD5.h. The correction for VH is simply the geometric mean of the co-polarized corrections (in linear units). This calibration offset is a constant and does not change with incidence angle or wind speed.

A polarization mixing adjustment [3] was applied to all the data, but the effects on both VV and VH are small and get weaker at the higher wind speeds [5].

Since IWRAP measures to the side of the aircraft, collocation between the nadir/aircraft sensors (e.g., SFMR, flight-level wind direction) and IWRAP was performed in two different ways within a hurricane. Each pass near the storm center was considered a "leg" of the flight, and for each leg a radius of maximum winds (RMW) was estimated from SFMR retrievals. Assuming a radially symmetric storm within twice the measured RMW, IWRAP and aircraft measurements were collocated in 0.5 km bins. Beyond this distance from the storm center, collocation was performed in 0.5 km bins of along-track distance. The assumption for the region outside twice the RMW is that the wind field is not significantly dynamic across the IWRAP beam. This also allows for proper binning of cells during downwind flight tracks. In both scenarios, the location of the IWRAP beam on the surface is used for the IWRAP measurement location.

To remove the strong wind-direction dependence from the co-polarized NRCS, the difference between the mean NRCS (A_0 term) and the NRCS observed was computed using the GMF from [3]. This difference was added to the IWRAP VV NRCS. Wind directions were obtained from the flight-level wind direction sensor and surface wind speeds were obtained from SFMR.

SFMR retrievals collocated with IWRAP are from the models described in [11]. The sensitivity of SFMR is questionable below 15 m s^{-1}, so only measurements with SFMR wind speeds above this level are used.

Rain rates were limited in a similar way to [5]: below 40 m s^{-1}, the maximum allowed rain rate was allowed to be 5 mm h^{-1}; above 40 m s^{-1}, the allowed rate was increased to 20 mm h^{-1}.

3. DISCUSSION

NRCS from incidence angles between 20° to 45° are shown in Figs. 1 and 2 with the same range on the vertical axes. Below 20° there is too much contamination from the strong nadir echo—due to the fields transmitted through antenna sidelobes—for a reliable incidence-angle dependence to be observed. Above 45° the signal-to-noise ratio is typically too low and the uncertainty in antenna gain too high for consistent measurements. This can start to be observed in the higher angle lines of Figs. 1 and 2.

Fig. 1 shows the mean VV NRCS response to ocean wind speed after excluding rainy data and adjusting for wind direction. The results show what the mean NRCS, or A_0 term of the typical $\sigma^0 = A_0\,(1 + a_1 \cos\chi + a_2 \cos 2\chi)$ ocean-surface NRCS signature. The A_0 results from [3] are shown as empty circles and labeled 'ws2015' in the legend. Similar consistency occurs between HH polarization NRCS and the model developed in [3], but are not shown for brevity.

The VH NRCS trends and levels in Fig. 2 with respect to wind speed match those in the recent literature [7], [8]. The data show a greater sensitivity to wind speed and a weaker sensitivity to incidence angle than the previous model developed from IWRAP data [3]. The incidence angle dependence is likely incorrect by a small amount; the higher incidence angles should have a smaller NRCS. While this could be due to noise, after performing this aggregation and analysis it has become clear that the antenna gain pattern for each season is critical and further improvement of this will be undertaken. A methodology is described in [12] that can be adapted to IWRAP.

4. CONCLUSIONS

The VV NRCS from hurricane seasons during which the IWRAP scatterometer collected data with the ESA antenna are consistent with the models developed in [3]. The VH NRCS do not show the same incidence angle or wind speed dependence as the model in [3], but the data is consistent with recent observations made by spaceborne synthetic aperture radar.

The incidence angle dependence of the VH NRCS need to be examined more closely, since they don't appear to match the inverse trend with incidence angle that is expected. This effect may be remedied by improving the antenna gain pattern estimation using an in-flight calibration method that is independent of a GMF.

This work is in progress and it is anticipated that we will be able to add data from winter seasons at a later step in the analysis.

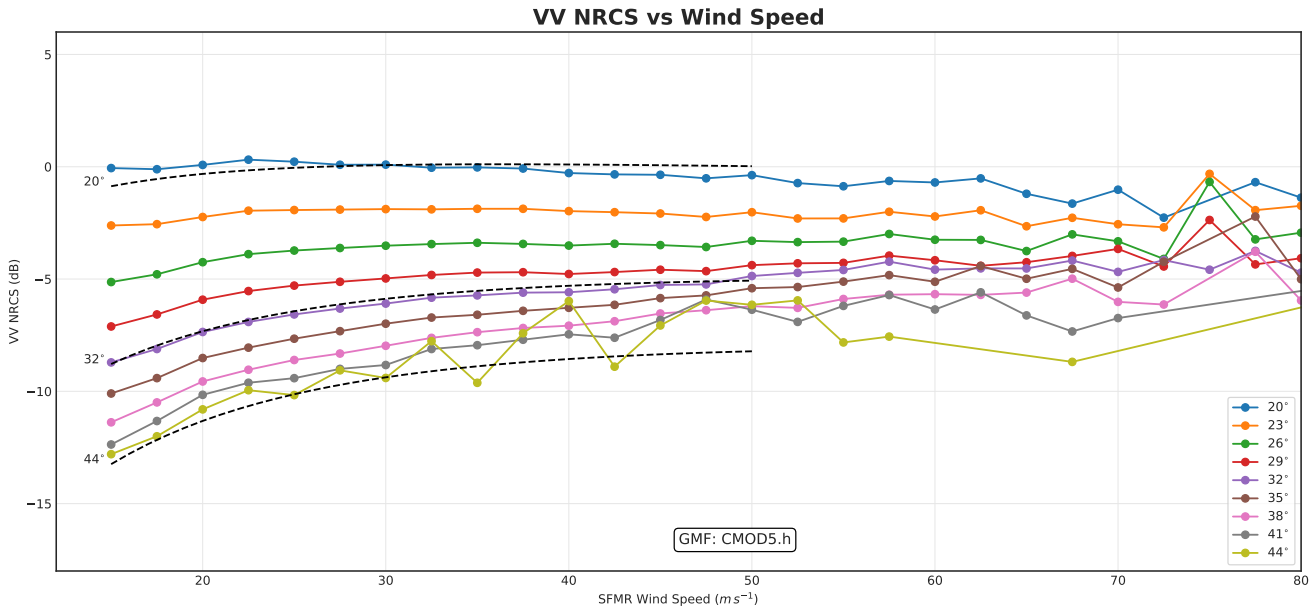

Fig. 1: Mean co-polarized (VV) NRCS in dB as a function of wind speed, adjusted for wind direction. Incidence angle values indicate measurements within ±0.5°. Data taken from within the RMW, in high rain rates, and at low SFMR wind speeds were excluded. Saturation at all incidence angles occurs at high winds. The GMF shown (CMOD5.h) is only valid up to 50 m s^{-1}. The wind direction adjustment was performed using CMOD5.h, the surface wind speed, and the flight-level wind direction.

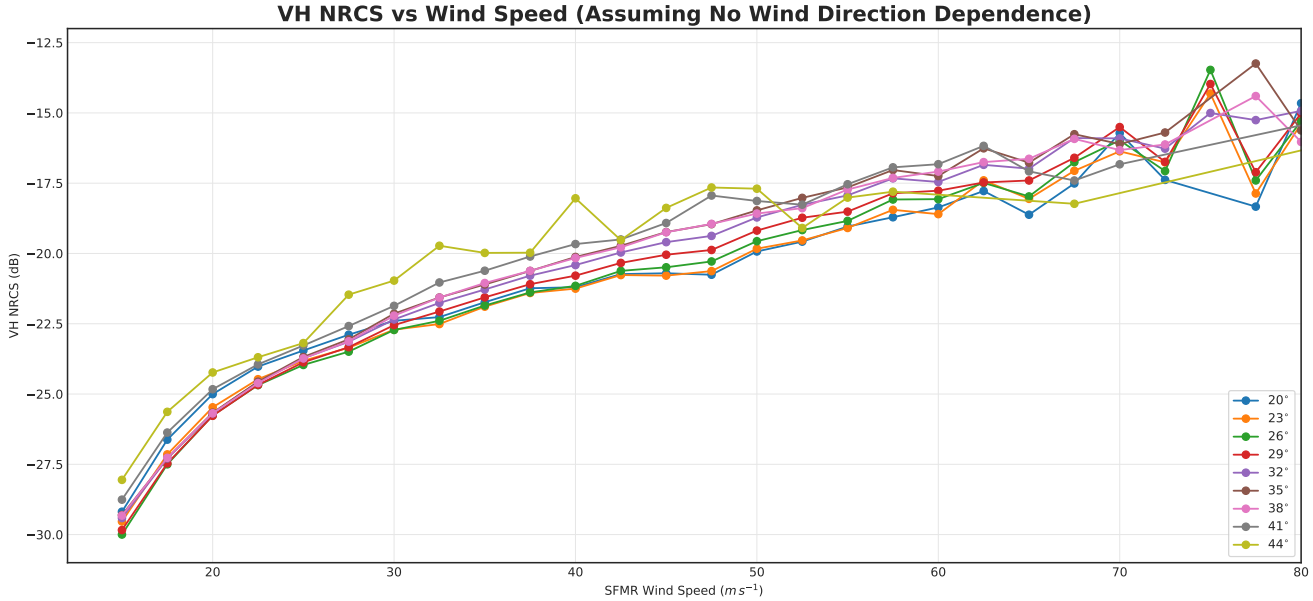

Fig. 2: Cross-polarized (VH) NRCS in dB as a function of wind speed. Incidence angle values indicate measurements within ±0.5°. Data taken from within the RMW, in high rain rates, and at low SFMR wind speeds were excluded. Saturation does not appear to occur at high wind speeds.

5. ACKNOWLEDGMENT

The authors thank the NOAA/NESDIS Ocean Remote Sensing Program for its support of their flight experiment program; the NOAA Hurricane Hunters and support staff at NOAA Aircraft Operations Center for their assistance in acquiring these data over the years; and the European Space Agency for loaning the antenna.

6. REFERENCES

[1] D. E. Fernandez, E. M. Kerr, A. Castells, J. R. Carswell, S. J. Shaffer, P. S. Chang, P. G. Black, and F. D. Marks, "IWRAP: The Imaging Wind and Rain Airborne Profiler for remote sensing of the ocean and the atmospheric boundary layer within tropical cyclones," *IEEE Transactions on Geoscience and Remote Sensing*, vol. 43, no. 8, pp. 1775–1787, Aug. 2005. DOI: 10.1109/TGRS.2005.851640.

[2] E. W. Uhlhorn, P. G. Black, J. L. Franklin, M. Goodberlet, J. Carswell, and A. S. Goldstein, "Hurricane Surface Wind Measurements from an Operational Stepped Frequency Microwave Radiometer," *Monthly Weather Review*, vol. 135, no. 9, pp. 3070–3085, 2007. DOI: 10.1175/MWR3454.1.

[3] J. W. Sapp, S. O. Alsweiss, Z. Jelenak, P. S. Chang, S. J. Frasier, and J. Carswell, "Airborne Co-polarization and Cross-Polarization Observations of the Ocean-Surface NRCS at C-Band," *IEEE Transactions on Geoscience and Remote Sensing*, vol. 54, no. 10, pp. 5975–5992, Jul. 7, 2016. DOI: 10.1109/TGRS.2016.2578048.

[4] J. Sapp, P. Chang, Z. Jelenak, S. Frasier, and T. Hartley, "Cross-polarized C-band sea-surface NRCS observations in extreme winds," in *Geoscience and Remote Sensing Symposium (IGARSS), 2016 IEEE International*, Beijing, China, 2016, pp. 2243–2246. DOI: 10.1109/IGARSS.2016.7729579.

[5] J. Sapp, Z. Jelenak, P. Chang, and S. Frasier, "C-Band Cross-Polarization Ocean Surface Observations in Hurricane Matthew," in *2018 IEEE International Geoscience and Remote Sensing Symposium (IGARSS)*, Jul. 2018, pp. 5595–5598. DOI: 10.1109/IGARSS.2018.8519433.

[6] P. Magnusson, P. Dimming, C. Lin, and A. Østergaard, "A thermally stable dual-polarized waveguide array," in *Proc. 9th EuCAP*, Lisbon, Portugal, Apr. 2015.

[7] P. A. Hwang, "Recent Development of Drag Coefficient, Foam, and Surface Roughness for High Wind EM Emission and Scattering Computation," in *IGARSS 2019 - 2019 IEEE International Geoscience and Remote Sensing Symposium*, Yokohama, Japan: IEEE, Jul. 2019, pp. 4622–4625. DOI: 10.1109/IGARSS.2019.8899020.

[8] A. Mouche, B. Chapron, J. Knaff, Y. Zhao, B. Zhang, and C. Combot, "Copolarized and Cross-Polarized SAR Measurements for High-Resolution Description of Major Hurricane Wind Structures: Application to Irma Category 5 Hurricane," *Journal of Geophysical Research: Oceans*, vol. 124, no. 6, pp. 3905–3922, 2019. DOI: 10.1029/2019JC015056.

[9] S. Soisuvarn, Z. Jelenak, P. S. Chang, S. O. Alsweiss, and Q. Zhu, "CMOD5.H—A High Wind Geophysical Model Function for C-Band Vertically Polarized Satellite Scatterometer Measurements," *IEEE Transactions on Geoscience and Remote Sensing*, vol. 51, no. 6, pp. 3744–3760, Jun. 2013. DOI: 10.1109/TGRS.2012.2219871.

[10] B. Zhang, W. Perrie, and Y. He, "Wind speed retrieval from RADARSAT-2 quad-polarization images using a new polarization ratio model," *Journal of Geophysical Research*, vol. 116, Aug. 4, 2011. DOI: 10.1029/2010JC006522.

[11] J. W. Sapp, S. O. Alsweiss, Z. Jelenak, P. S. Chang, and J. Carswell, "Stepped Frequency Microwave Radiometer Wind-Speed Retrieval Improvements," *Remote Sensing*, vol. 11, no. 3, p. 214, Jan. 22, 2019. DOI: 10.3390/rs11030214.

[12] R. K. Hawkins, "Determination of antenna elevation pattern for airborne SAR using the rough target approach," *IEEE Transactions on Geoscience and Remote Sensing*, vol. 28, no. 5, pp. 896–905, Sep. 1990. DOI: 10.1109/36.58979.